

Appearance of Successive Phase Transition in $\text{SmRu}_4\text{P}_{12}$ under High Magnetic Fields Probed by ^{31}P Nuclear Magnetic Resonance

Kenichi HACHITANI^{1,2*}, Hideaki AMANUMA¹, Hideto FUKAZAWA^{1,3}, Yoh KOHORI^{1,3},
Keiichi KOYAMA⁴, Ken-ichi KUMAGAI⁵, Chihiro SEKINE⁶ and Ichimin SHIROTANI⁶

¹ Graduate School of Science and Technology, Chiba University, Chiba 263-8522

² Advanced Meson Science Laboratory, RIKEN (The Institute of Physical and Chemical Research), Wako, Saitama 351-0198

³ Department of Physics, Faculty of Science, Chiba University, Chiba 263-8522

⁴ High Field Laboratory for Superconducting Materials, Institute for Materials Research, Tohoku University, Sendai 980-8577

⁵ Division of Physics, Graduate School of Science, Hokkaido University, Sapporo 060-0810

⁶ Department of Electrical and Electronic Engineering, Muroran Institute of Technology, Muroran, Hokkaido 050-8585

The ^{31}P -NMR (nuclear magnetic resonance) measurements of the filled skutterudite $\text{SmRu}_4\text{P}_{12}$ have been carried out in several applied magnetic fields. The line width of the ^{31}P -NMR spectrum rapidly increases below the metal-insulator transition temperature T_{MI} , which indicates the appearance of an internal field below the temperature. Though no distinct anomaly was observed below T_{MI} in low fields, a complicated structure was observed between the Néel temperature T_{N} and T_{MI} ($T_{\text{N}} < T_{\text{MI}}$) above 70 kOe. The spin-lattice relaxation rate $1/T_1$ is almost independent of temperature above T_{MI} , and rapidly decreases below T_{MI} . The $1/T_1$ in low fields decreases monotonously, whereas the strong suppression of $1/T_1$ occurs between T_{N} and T_{MI} above 70 kOe. The structure of the spectra and the suppression of $1/T_1$ become apparent with increasing field.

KEYWORDS: $\text{SmRu}_4\text{P}_{12}$, Filled skutterudite, Metal-insulator (M-I) transition, Multipolar (octupolar) order, Antiferromagnetic (AFM) order, ^{31}P -NMR (nuclear magnetic resonance)

1. Introduction

Filled skutterudites RT_4X_{12} (R : rare earth, actinide; T : Fe, Ru, Os; X : P, As, Sb) show a wide variety of physical properties.¹⁻⁷ Remarkable phenomena observed in these systems are caused by the combination of the strong hybridization effect between the p-conduction and the f-localized electrons, the unique band structure, the orbital degree of freedom of the R ions and the crystalline electric field (CEF) effect. Among them, $\text{PrRu}_4\text{P}_{12}$ and $\text{SmRu}_4\text{P}_{12}$ exhibit metal-insulator (M-I) transitions at the temperatures T_{MI} of 62 K and 16.5 K, respectively.^{5,8} The M-I transition in $\text{PrRu}_4\text{P}_{12}$ is a non-magnetic one caused by the band nesting. On the other hand, the M-I transition in $\text{SmRu}_4\text{P}_{12}$ accompanies a magnetic anomaly. Different features of each M-I transition have attracted much attention.

The T_{MI} of $\text{SmRu}_4\text{P}_{12}$ exhibits the characteristic magnetic field dependence.^{9,10} It increases with increasing field up to 200 kOe, and saturates around 300 kOe. The reentrant behavior is expected at higher fields. In addition, it is considered that an extra phase transition occurs at 15 K in zero field.^{9,10} The transition temperature which is called T_{N} decreases monotonously with increasing field. Though the associate anomaly is indistinct in low fields, it gradually becomes apparent with increasing field. The behavior is similar to that of CeB_6 where an antiferro-quadrupolar (AFQ) order and a subsequent antiferromagnetic (AFM) order occur.¹¹ Hence, the successive transition in $\text{SmRu}_4\text{P}_{12}$ had been expected to be the AFQ order below T_{MI} (the phase I above T_{MI} and the phase II between T_{N} and T_{MI}) and the AFM order

below T_{N} (phase III), respectively.

On the contrary, recent ultrasonic measurements have shown that the elastic constant of $\text{SmRu}_4\text{P}_{12}$ exhibits a slight and a large softening above T_{MI} and below T_{MI} toward T_{N} , respectively.^{12,13} The softening above T_{MI} is much smaller than that expected for the case of the AFQ order where the quadrupole-quadrupole interaction plays an important role.¹³ From group theoretical considerations, the octupolar (Γ_{5u}) order below T_{MI} and the AFM (Γ_{4u}) one below T_{N} are the most probable candidates for the order parameters of the phase II and III, respectively.¹³ There is a clear difference between the AFQ order and the octupolar order in zero field. The AFQ order is non-magnetic and holds the time reversal symmetry. On the contrary, the octupolar order is magnetic one which spontaneously breaks the symmetry. Zero field and longitudinal fields μSR measurements have shown the appearance of a static internal field below T_{MI} , which excludes the occurrence of the AFQ order in the phase II.^{14,15} Indeed, it is theoretically pointed out with multi-orbital Anderson model calculations that the Γ_{5u} and the Γ_{4u} octupolar fluctuations can become significant in Sm-based filled skutterudite systems.¹⁶

It is required to determine the order parameters of the phase II and III in $\text{SmRu}_4\text{P}_{12}$. In order to clarify the physical properties of this system, it is important to understand the CEF effect. Here, we have carried out ^{31}P -NMR (nuclear magnetic resonance) of $\text{SmRu}_4\text{P}_{12}$ in several applied magnetic fields in order to investigate the system microscopically. In this paper, we report the results of the measurements below T_{MI} including that at high temperatures above T_{MI} .

*E-mail address: hachitani@physics.s.chiba-u.ac.jp

2. Experimental

The single-phase polycrystalline $\text{SmRu}_4\text{P}_{12}$ was synthesized by using the high temperature and high pressure method.⁸⁾ The sample was crushed into powder for the experiments. The ^{31}P -NMR experiments have been carried out by using phase-coherent pulsed NMR spectrometers and superconducting magnets. The NMR spectra were measured both by sweeping the applied fields at a constant resonance frequency and by sweeping the resonance frequency at a constant applied field. The spin-lattice relaxation rate $1/T_1$ was measured with the saturation recovery method in applied fields. The nuclear magnetization recovery curve was fitted by a simple exponential function as expected for the nuclear spin $I = 1/2$ of the ^{31}P nucleus. The experiment in the field of 150 kOe was performed at High Field Laboratory for Superconducting Materials, Institute for Materials Research, Tohoku University.

3. Results

3.1 ^{31}P -NMR spectra above T_{MI}

Figure 1 shows the frequency swept ^{31}P -NMR spectra at several temperatures T above T_{MI} in the field of 94.063 kOe. The line width of the spectra increases with decreasing temperature and with increasing field. The spectra above about 70 K show a typical powder pattern with the uniaxial Knight shift distribution for the nuclear spin $I = 1/2$. Below about 70 K, the uniaxial symmetry gradually decreases with decreasing temperature. The ^{31}P -NMR spectra were analyzed by taking into account of the powder average of the Knight shift K anisotropy and the excess Gaussian broadening. The K is expressed as

$$K = K_{\text{iso}} + K_{\text{ax}}(3 \cos^2 \theta - 1) - K_{\text{aniso}}(\sin^2 \theta \cos 2\phi), \quad (1)$$

where K_{iso} , K_{ax} and K_{aniso} represent an isotropic term, a uniaxial term and the deviation from the uniaxial symmetry, respectively.

Figure 2 shows the bulk susceptibility χ dependence of K_{iso} (K - χ plot). The K_{iso} almost follows the liner function of the χ expressed by the formula

$$K_{\text{iso}} = \frac{A_{\text{hf}}}{N_A \mu_B} \chi, \quad (2)$$

where N_A and μ_B are the Avogadro constant and the Bohr magneton, respectively. The hyperfine coupling constant $A_{\text{hf}} \simeq 2.7 \text{ kOe}/\mu_B$ was estimated from the slope of the solid line shown in Fig. 2. This value is consistent with a previous result.¹⁷⁾

Figure 3 shows the T dependence of K_{ax} and K_{aniso} . The K_{ax} has the weak T dependence in the whole T region with the value of about 0.013 %. The K_{aniso} decreases with increasing temperature below about 70 K, and decreases very gradually at higher temperatures (0.0044 % at 292 K). One origin of the anisotropic hyperfine coupling is the the direct dipoler coupling of Sm^{3+} magnetic moments and ^{31}P nuclear spins. The lattice sum calculation predicts nearly uniaxial Knight shift to be $K_{\text{ax}} \simeq 0.007 \%$ and $K_{\text{aniso}} \simeq 0.0008 \%$ at 292 K. These results are shown in Table I including the experimental results. This indicates that half of the anisotropic

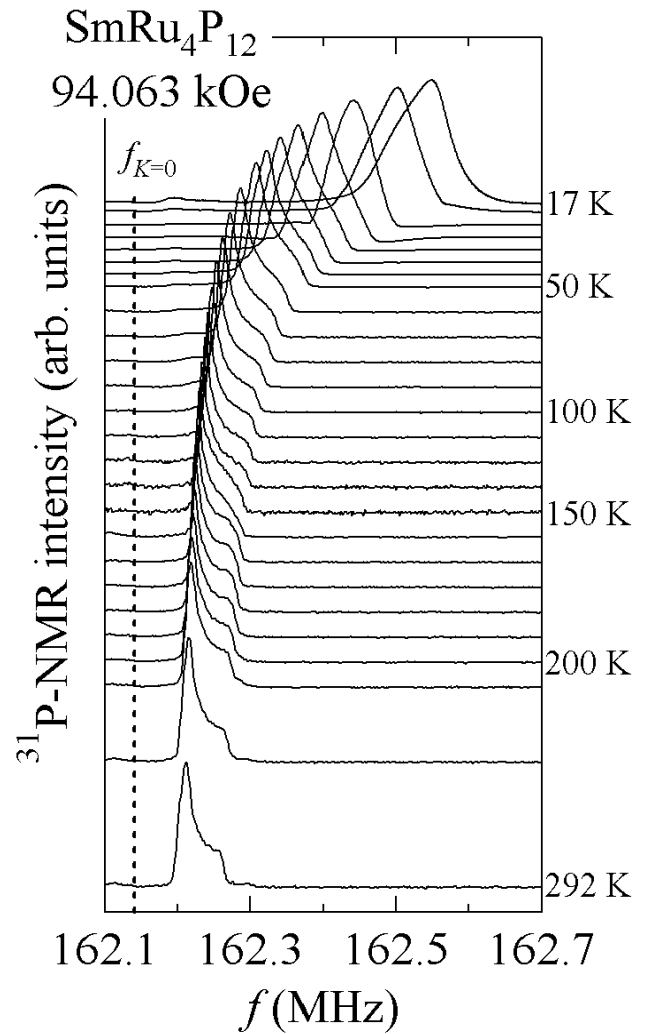


Fig. 1. Resonance frequency swept ^{31}P -NMR spectra at several temperatures above T_{MI} in the applied magnetic field of 94.063 kOe. The broken line shows the frequency of 162.14 MHz at $K = 0$ estimated from the nuclear gyro-magnetic ratio of the ^{31}P nucleus.

hyperfine coupling can be explained by the direct dipolar coupling of the Sm^{3+} magnetic moments and the ^{31}P nuclear spins. An anisotropic field via the dipolar coupling of P-3p spins and ^{31}P nuclei induced by spin polarizations at the P-3p spins makes an extra contribution for the anisotropic hyperfine coupling.¹⁸⁾ The sum of these contributions would explain the observed values. The change of the ^{31}P -NMR spectra below about 70 K is represented by the increase of K_{aniso} , which would be due to that the change of Sm-4f orbital shape occurs associated with the thermal excitation of the CEF levels. This is consistent with the result that the CEF level splitting between the ground state Γ_5 and the excited Γ_{67} of 60 K was estimated from a specific heat measurement.¹⁹⁾

3.2 ^{31}P -NMR spectra below T_{MI}

The field swept ^{31}P -NMR spectra at several temperatures below T_{MI} at the frequencies of 9.23, 46.268 and 123.979 MHz are shown in Figs. 4 (a), (b) and (c), respectively. The shape of the spectra at 9.23 and 46.268 MHz

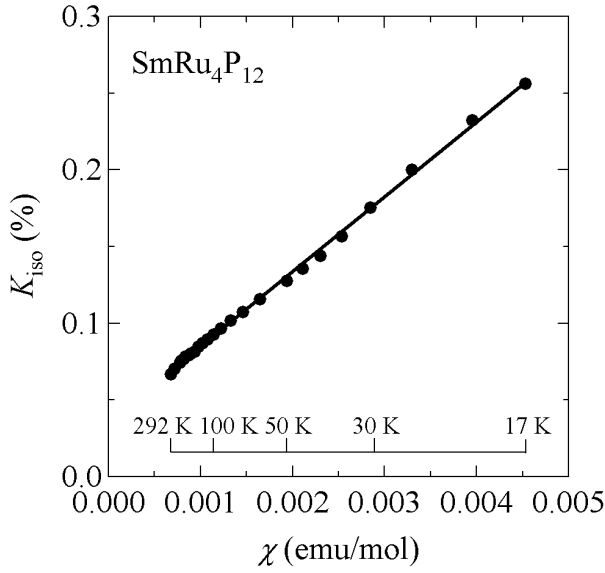


Fig. 2. Bulk susceptibility dependence of K_{iso} (K - χ plot). The solid line shows the best-fit result by the formula (2). Some temperatures are also shown corresponding to χ .

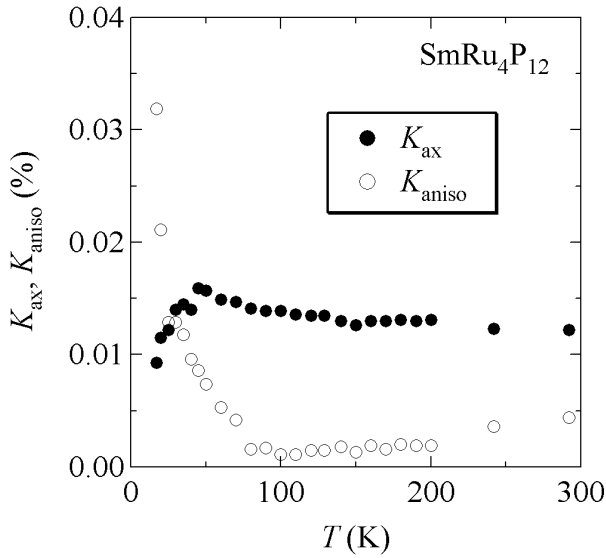


Fig. 3. Temperature dependence of K_{ax} (closed circles) and K_{aniso} (open circles).

(corresponding to the fields of about 5.5 and 27 kOe, respectively) have a triangle-like powder pattern. The previously obtained ^{31}P -NMR spectra at 17 MHz also have a similar triangle-like feature.¹⁷⁾ The spectrum of $\text{SmRu}_4\text{P}_{12}$ is quite different from that of a simple AFM $\text{SmOs}_4\text{P}_{12}$ with T_N of 4.6 K as seen in Fig. 4 (d). In the case of $\text{SmOs}_4\text{P}_{12}$ which has a homogeneous AFM structure, the spectra have a rectangle-type powder pattern.²⁰⁾ The zero field μSR spectra of $\text{SmRu}_4\text{P}_{12}$ also suggest that the spin alignment is not so coherent.¹⁴⁾ The muon-spin precession was not clearly observed in $\text{SmRu}_4\text{P}_{12}$, whereas it was clearly observed in the case of $\text{SmFe}_4\text{P}_{12}$ and $\text{SmOs}_4\text{P}_{12}$ which have magnetically

Table I. Experimental and the dipolar calculated values of K_{ax} and K_{aniso} at the temperature of 292 K.

	K_{ax} (%)	K_{aniso} (%)
Experimental	0.012	0.0044
Calculated	0.007	0.0008

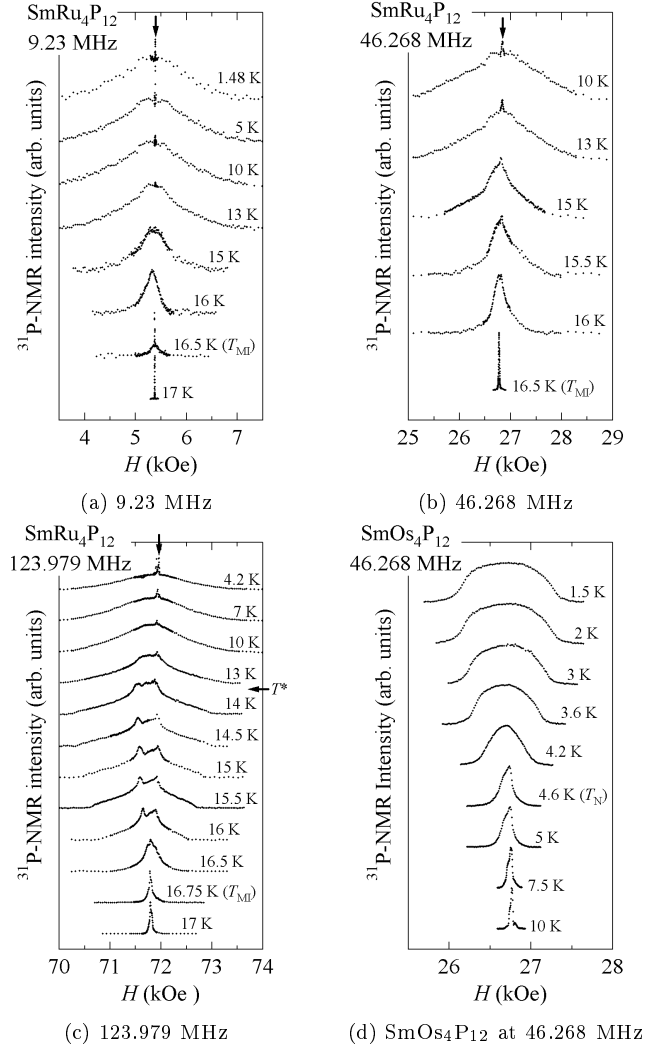


Fig. 4. Applied magnetic field swept ^{31}P -NMR spectra of $\text{SmRu}_4\text{P}_{12}$ at several temperatures below T_{MI} at the resonance frequencies of (a) 9.23, (b) 46.268 and (c) 123.979 MHz. The rather sharp signals pointed by the arrows in each figure arises from impurity phases with spurious ^{31}P nuclei. The spectra of $\text{SmOs}_4\text{P}_{12}$ at 46.268 MHz are shown in (d).

ordered ground states.^{14,21)} These results indicate the existence of an inhomogeneously distributed transferred hyperfine field in $\text{SmRu}_4\text{P}_{12}$, which reflects a non-simple magnetic structure such as an incommensurate structure.

With increasing field, the fine structure is induced by the fields around the center of the resonance line, as seen in the spectra at 123.979 MHz (corresponding to the field of about 72 kOe) in Fig. 4 (c). The shape of the spectra is not a simple triangle-like but much complicated pattern in the intermediate T range between T^* (about 13.5 K) and T_{MI} . Here, T^* was determined from the anomalies

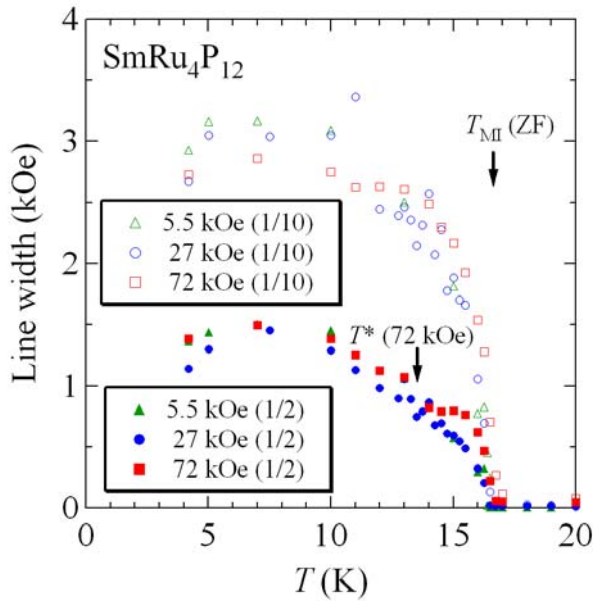


Fig. 5. Temperature dependence of the line width in several applied magnetic fields, which were estimated from the full width at half maximum (1/2) and at one-tenth maximum (1/10) values of the ^{31}P -NMR spectra in Fig. 4 (a), (b) and (c), respectively.

observed in $1/T_1$ which is discussed later in the next section.

Figure 5 shows the T dependence of the line width in several fields estimated from the full width at half maximum and at one-tenth maximum values of the ^{31}P -NMR spectra in Figs. 4 (a), (b) and (c), respectively. The line width rapidly increases below T_{MI} , which indicates that an internal field at the ^{31}P site develops just below T_{MI} . The internal fields at 5.5 and 27 kOe are independent of the field in low fields. The T dependence of the internal field at 72 kOe is different from that in low fields, which associates the appearance of the fine structure. No anomaly was observed in low fields around T^* . Since the field dependence is very small, the T dependence of the internal field estimated from ^{31}P -NMR is consistent with the previous μSR result which indicates the magnetic order below T_{MI} .¹⁴⁾

The field induced anomaly of the ^{31}P -NMR spectra is enhanced in higher fields, as seen in Fig. 6, where the frequency swept spectra at the fields of 94.063 and 147.2 kOe (corresponding to the frequencies of about 162 and 254 MHz, respectively) T_{MI} are shown. In frequency swept spectra of wide resonance lines, the NMR signal often distorted owing to the technical reason, *i.e.*, the small impedance mismatch of the network makes rf reflection, which affects the shape of the spectra. In our case, the line width of 3-5 MHz is not so broad for getting the structure of the resonance lines. The separation of the fine structure below increases with increasing field.

A previously reported ^{31}P -NMR result showed typical spectra with two trapezoid in shape below T_{MI} ,²²⁾ which is different from the triangle-like one in our case. Our sample is a polycrystal synthesized by the high temperature and high pressure method,⁸⁾ and a grain of the

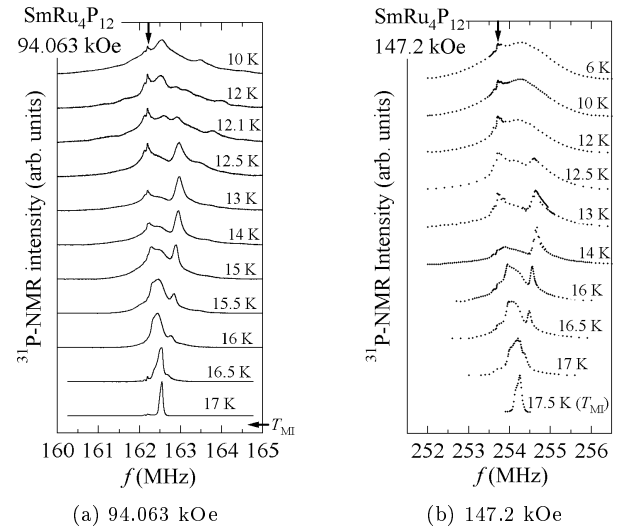


Fig. 6. Resonance frequency swept ^{31}P -NMR spectra at several temperatures below T_{MI} in the applied magnetic fields of (a) 94.063 and (b) 147.2 kOe. The rather sharp signals pointed by the arrows in each figure arises from impurity phases with spurious ^{31}P nuclei.

powdered samples would include a lot of domains. Hence, the sample orients randomly to the fields in our measurement. Indeed, our ^{31}P -NMR spectra above T_{MI} show a typical uniaxial powder pattern as seen in Fig. 1. On the other hand, the sample pieces of the previous report consist of many small single crystals, and they were moderately crushed.²²⁾ Then, the previously reported spectra would be obtained in a partially oriented sample condition. We consider that the difference of them arises from the crystal orientation to applied fields.

3.3 Spin-lattice relaxation rate $1/T_1$

Figures 7 and 8 show the T dependence of $1/T_1$ in several fields. The T dependence of $1/T_1$ of the non-magnetic $\text{LaRu}_4\text{P}_{12}$ is also shown in Fig. 7 as a reference.¹⁷⁾ The $1/T_1$ of $\text{SmRu}_4\text{P}_{12}$ is nearly T independent above T_{MI} , where $1/T_1$ is dominated by the fluctuations of Sm^{3+} 4f-localized moments. The $1/T_1$ rapidly decreases below T_{MI} , and becomes nearly proportional to T below about 3.5 K. The measured $1/T_1$ is the sum of the transferred contribution at the ^{31}P site from Sm^{3+} 4f-localized and from conduction electrons. In the low T region ($1/T_1 \propto T$), the latter has a dominant contribution. The value of $1/T_1 T$ below 3.5 K is about 15 % of that of $\text{LaRu}_4\text{P}_{12}$, which indicates decrease of the density of states of the conduction electrons at ^{31}P site associated with the M-I transition. The T dependence of the $1/T_1$ is monotonous at low fields where no indistinct anomaly was observed around T^* . After subtracting the onsite (^{31}P site) contribution, the T dependence of $1/T_1$ at low temperatures is nearly exponential. On the basis of the Raman scattering by two magnons, the energy gap of about 50 K was estimated.²³⁾ This value is consistent with the previous ^{31}P -NMR result and half of that obtained from an optical spectroscopy measurement.^{17, 24)}

With increase field, the strong suppression of $1/T_1$ appears in the T region between T^* and T_{MI} , as shown in

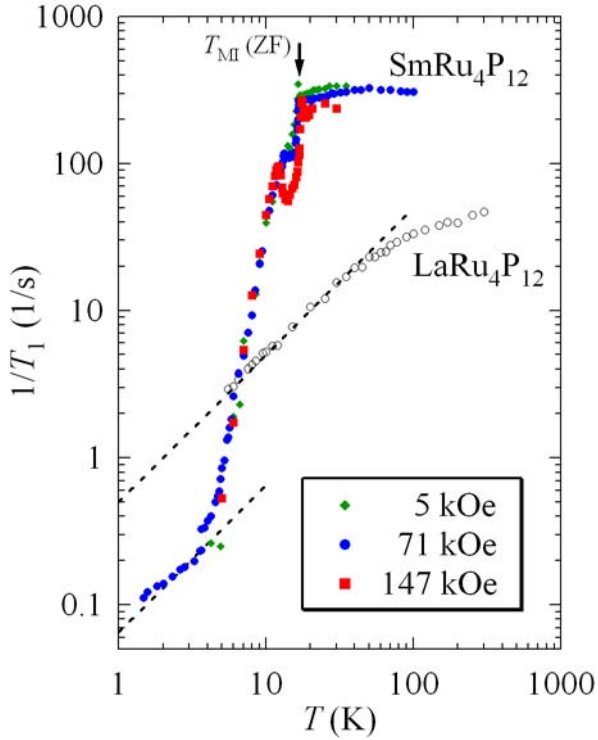


Fig. 7. Temperature dependence of $1/T_1$ in several applied magnetic fields. The $1/T_1$ of the non-magnetic $\text{LaRu}_4\text{P}_{12}$ is also shown as a reference.¹⁷⁾ The broken lines show guide to the eyes for the Korringa behavior ($1/T_1 \propto T$).

Fig. 8. The field induced phase transition at T^* becomes apparent above 70 kOe,²²⁾ and the anomaly enhanced with increasing field. At the field of 147 kOe, the critical slowing-down behavior were observed around both T^* and T_{MI} . Between T^* and T_{MI} above 70 kOe where the spectra have the structure, $1/T_1$ were measured at the frequency of the line center of the spectrum just above T_{MI} . The frequency locates between the two peaks of the structure, and corresponds to the peak of the triangle-like spectra below T^* . The behavior of $1/T_1$ is nearly the same as that obtained at two peaks of the structure.

4. Discussion

The T dependence of both the ^{31}P -NMR spectra and $1/T_1$ in various fields have demonstrated that the sharp anomaly at T_{MI} shifts to higher T with increasing field. On the contrary, the round anomaly at T^* , which is undetectably small in low fields, becomes gradually apparent and shifts to lower T with increasing field. The behavior is similar to that observed in other measurements.^{9,10,12,13)} The field-temperature (H - T) phase diagram obtained from ^{31}P -NMR is shown in Fig. 9. The T_{MI} coincides with other data, whereas T^* obtained from $1/T_1$ is lower than T_{N} corresponding to the anomalies obtained from other macroscopic measurements.^{9,10)} Though the reason of this behavior is not clear at the moment, the similar tendency also appears in the previous elastic constant result.¹³⁾ As a result, the T^* obtained from ^{31}P -NMR is considered to be T_{N} .

The appearance of an internal field below T_{MI} in low

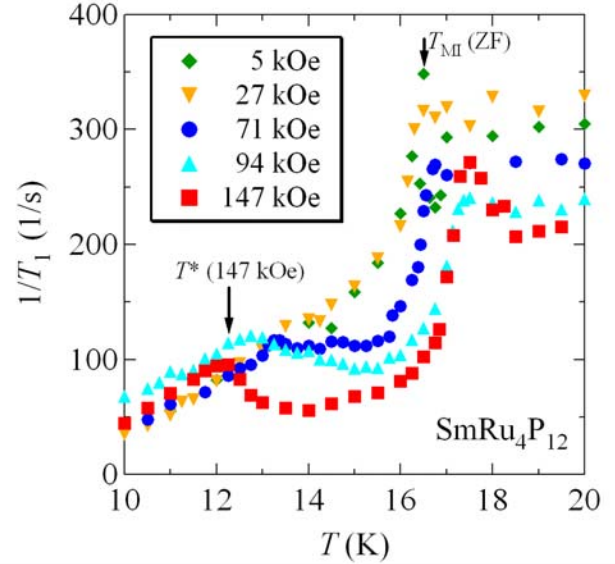


Fig. 8. Temperature dependence of $1/T_1$ in several applied magnetic fields around T_{MI} and T_{N} , which was obtained by expanding Fig. 7.

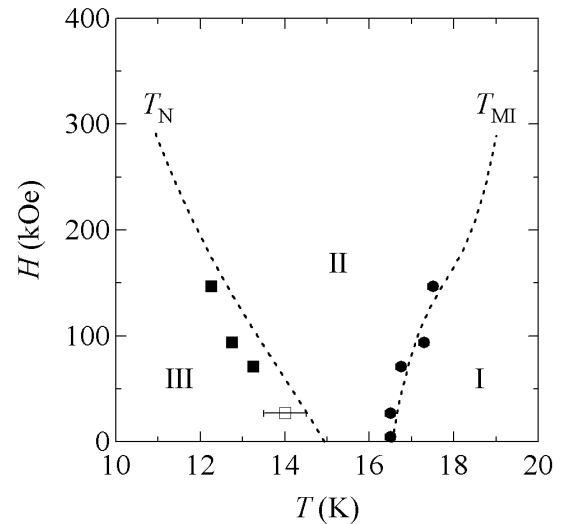


Fig. 9. H - T phase diagram of $\text{SmRu}_4\text{P}_{12}$ obtained from ^{31}P -NMR. The circles show T_{MI} , and the squares show T^* . The open square means that the anomaly is not so apparent. The broken lines are obtained from macroscopic measurements.¹⁰⁾

fields shows that the phase transition at T_{MI} is a spontaneous magnetic transition but not an induced one. It is noted that the internal field obtained from μSR and from the low field ^{31}P -NMR are essentially the same. A field induced anomaly around T_{N} were observed in both spectra and $1/T_1$ above 70 kOe. The $1/T_1$ between T_{N} and T_{MI} is sensitive to fields, whereas the effects of fields are small below T_{N} .

The magnetic transition occurs below T_{MI} , where a dipolar or octupolar order is responsible for the phase transition. One of the aspects of this system is the complicated magnetic field response. An orbital contribution

seems to have an important role. The ground state of $\text{SmRu}_4\text{P}_{12}$ is Γ_{67} of the cubic T_h symmetry,¹⁹⁾ which corresponds to Γ_8 state of the cubic O_h symmetry. A scenario was proposed to account for the above phenomena with the second order transitions at T_{MI} and T_{N} .¹³⁾ Among dipole, quadrupole and octupole moments in T_h symmetry, the possible scenario is as follows. The phase III is a magnetic order of a dipole moment, which was well established by μSR , ^{31}P -NMR and a ^{149}Sm nuclear resonant forward scattering measurement.^{14, 15, 17, 22, 25)} Then, a possible candidate for the order parameter of the phase II is the octupole moment of T_i^β ($i = x, y, z$), which connects the phases II and III with the second order transition.¹³⁾ This model successfully explains the indistinct phase transition at T_{N} in low fields through the mixing of Γ_{4u} and Γ_{5u} in T_h symmetry, which does not mix in the O_h symmetry.

Further measurements including the neutron diffraction are highly expected for the further understanding of the complicated properties of $\text{SmRu}_4\text{P}_{12}$. The ^{31}P -NMR with one single crystal is also expected to provide the accurate information for the complicated structure of the spectra.

5. Summary

In summary, ^{31}P -NMR of the filled skutterudite $\text{SmRu}_4\text{P}_{12}$ has been carried out in several fields. The line width of the ^{31}P -NMR spectra rapidly increases below T_{MI} . In low fields, the effect of the field is small, and the internal field increases monotonously. On the contrary, the field induced anomaly becomes apparent with increasing field between T_{N} and T_{MI} . The T dependence of $1/T_1$ shows a gradual decrease in low fields, and successive anomaly at T^* and T_{MI} in high fields.

Acknowledgment

The authors would like to thank T. Goto, M. Yoshizawa, K. Matsuhira, T. Hotta and S. Tsutsui for their useful discussions. This work was supported by a Grant-in-Aid for Scientific Research from the Ministry of Education, Sport, Science and Culture of Japan (no. 17740212). The work at Muroran Institute of Technology was supported by a Grant-in-Aid for Scientific Research in Priority Area "Skutterudite" (no. 15072201) of the Ministry of Education, Culture, Sports, Science and Technology, Japan.

1) W. Jeitschko and D. Braun: Acta Crystallogr. Sect. B **33** (1977) 3401.

- 2) F. Grandjean, A. Gerard, D. J. Braung and W. Jeitschko: J. Phys. Chem. Solids **45** (1984) 877.
- 3) M. S. Torikachvili, J. W. Chen, Y. Dalichaouch, R. P. Guertin, M. W. McElfresh, C. Rossel, M. B. Maple and G. P. Meisner, Phys. Rev. B **36** (1987) 8660.
- 4) I. Shirovani, T. Uchiyumi, K. Ohno, C. Sekine, Y. Nakazawa, K. Kanoda, S. Todo and T. Yagi: Phys. Rev. B **56** (1997) 7866.
- 5) C. Sekine, T. Uchiyumi, I. Shirovani and T. Yagi: Phys. Rev. Lett. **79** (1997) 3218.
- 6) D. A. Gajewski, N. R. Dilley, E. D. Bauer, E. J. Freeman, R. Chau, M. B. Maple, D. Mandrus, B. C. Sales and A. H. Lacerda: J. Phys.: Condens. Matter **10** (1998) 6973.
- 7) N. Takeda and M. Ishikawa: J. Phys.: Condens. Matter **13** (2001) 5971.
- 8) C. Sekine, T. Uchiyumi, I. Shirovani and T. Yagi: *Science and Technology of High Pressure*, ed. M. H. Manghnant *et al.* (Universities Press, Hyderabad, 2000) p. 826.
- 9) K. Matsuhira, Y. Hinatsu, C. Sekine, T. Togashi, H. Maki, I. Shirovani, H. Kitazawa, T. Takamasu, G. Kido: J. Phys. Soc. Jpn. **71** Suppl. (2002) 237.
- 10) C. Sekine, I. Shirovani, K. Matsuhira, P. Haen, S. De Brion, G. Chouteau, H. Suzuki and H. Kitazawa: Acta Phys. Pol. B **34** (2003) 983.
- 11) J. M. Effantin, J. Rossat-Mignod, P. Bulet, H. Bartholin, S. Kunii and T. Kasuya: J. Magn. Magn. Mater. **47&48** (1985) 145.
- 12) M. Yoshizawa, Y. Nakanishi, T. Kumagai, M. Oikawa, C. Sekine and I. Shirovani: J. Phys. Soc. Jpn. **73** (2004) 315.
- 13) M. Yoshizawa, Y. Nakanishi, M. Oikawa, C. Sekine, I. Shirovani, S. R. Saha, H. Sugawara and H. Sato: J. Phys. Soc. Jpn. **74** (2005) 2141.
- 14) K. Hachitani, H. Fukazawa, Y. Kohori, I. Watanabe, C. Sekine and I. Shirovani: Phys. Rev. B **73** (2006) 052408.
- 15) K. Hachitani, H. Amanuma, H. Fukazawa, Y. Kohori, I. Watanabe, K. Kumagai, C. Sekine, I. Shirovani: J. Phys. Soc. Jpn. **75** Suppl. (2006) 164.
- 16) T. Hotta: J. Phys. Soc. Jpn. **74** (2005) 2425.
- 17) K. Fujiwara, K. Ishihara, K. Miyoshi, J. Takeuchi, C. Sekine and I. Shirovani: Physica B **329-333** (2003) 476.
- 18) A. Abragam: *The Principles of Nuclear Magnetic Resonance* (Clarendon Press, Oxford, 1961) p. 205.
- 19) K. Matsuhira, Y. Doi, M. Wakeshima, Y. Hinatsu, H. Amitsuka, Y. Shimaya, R. Giri, C. Sekine and I. Shirovani: J. Phys. Soc. Jpn. **74** (2005) 1030.
- 20) K. Hachitani, H. Fukazawa, Y. Kohori, I. Watanabe, K. Kumagai, C. Sekine and I. Shirovani: Physica B **378-380** (2003) 230.
- 21) K. Hachitani, H. Fukazawa, Y. Kohori, Y. Yoshimitsu, K. Kumagai, I. Watanabe, R. Giri, C. Sekine and I. Shirovani: *IPAP Conf. Series 5* (2004) 37.
- 22) S. Masaki, T. Mito, N. Oki, S. Wada and N. Takeda: J. Phys. Soc. Jpn., **75** (2006) 053708.
- 23) T. Moriya: Prog. Theor. Phys. **16** (1956) 23, 641.
- 24) M. Matsunami, L. Chen, M. Takimoto, H. Okamura and T. Nanba: Phys. Rev. B **72** (2005) 073105.
- 25) S. Tsutsui, Y. Kobayashi, T. Okada, H. Haba, H. Onodera, Y. Yoda, M. Mizumaki, H. Tanida, T. Uruga, C. Sekine, I. Shirovani, D. Kikuchi, H. Sugawara and H. Sato: J. Phys. Soc. Jpn. **75** (2006) 093703.